

Supporting Information

for

Self-assembly and activation of a titania-nanotube based photocatalyst for H₂ evolution

Fan Fu,^{ab} Zhenni Wu,^a Gihoon Cha^a and Patrik Schmuki^{*ac}

^aDepartment of Materials Science WW-4, LKO, University of Erlangen-Nuremberg,
Martensstrasse 7, 91058 Erlangen, Germany;

^bNational Engineering Laboratory for Modern Silk, College of Textile and Clothing
Engineering, Soochow University, Suzhou 215123, PR China;

^cRegional Centre of Advanced Technologies and Materials, Faculty of Science, Palacký
University Olomouc, Šlechtitelů 27, 783 71 Olomouc, Czech Republic.

* Corresponding author: schmuki@ww.uni-erlangen.de

Experimental details:

Preparing of TiO₂ nanotube layers

Self-organized TiO₂ nanotubes were grown from titanium foil (1 mm, Advent, 99.8%) by electrochemical anodization. Before anodization, Ti foil was cleaned in an ultrasonic bath with acetone, ethanol, and deionized water for 15 minutes each, and then dried by N₂ stream. The anodization process was carried out in a traditional two-electrode configuration system that uses Ti foil as the working electrode and platinum plate as

the counter electrode. It was performed in an EG (ethylene glycol, 99.5% purity, Carl Roth)-based electrolyte which additionally contains NH_4F (0.15 M, 98% purity, Carl Roth) and deionized H_2O (3 vol%). A two-step anodization process was employed under a voltage of 60 V to get a highly aligned TiO_2 nanotube array. The first anodization was carried out for 20 minutes, creating well-ordered etch ditches in the Ti substrate. Subsequently, the formed TiO_2 nanotube layer was removed by a sonicator gun, followed by DI water rinsing and N_2 stream drying. Then the foil was anodized for a second time for 14 min to reach approximately 7 μm of tube length. Eventually, the foil with TiO_2 nanotubes was immersed in ethanol for 5 minutes and rinsed by ethanol to remove surface residual electrolyte, and dried in N_2 flow.

Annealing process

Water annealing of as-formed TiO_2 nanotubes was achieved during photocatalytic H_2 evolution by bathing the reaction cell in 50 °C water. In order to get a fully crystalline anatase phase, thermal annealing of the as-formed TiO_2 nanotubes was performed in air at 450 °C for 1 hour.

Characterization

The morphology and structure of the TiO_2 nanotubes were studied by field-emission scanning electron microscopy (SEM, S-4800, Hitachi, Japan). To identify the chemical composition of the obtained samples, an X-ray photoelectron spectrometer (XPS, PHI 5600, US) and energy-dispersive X-ray analysis (EDAX, fitted for S-4800, Genesis) were used. The calibration peak used was Ti 2p at 486 eV. The crystallinity of TiO_2

nanotubes was investigated via X-ray diffraction (XRD, X'pert Philips PMD diffractometer) which was equipped with a Panalytical X'celerator detector and the XRD patterns were taken using graphite monochromized Cu irradiation (wavelength: 0.154056 nm). UV-Vis absorption spectra of reaction solution were recorded by UV-Vis absorption spectrometer (Lambda Bio XLS, PerkinElmer). Incident photon-to-current conversion efficiency (IPCE) spectra were recorded at a constant potential of 0.5 V vs. Ag/AgCl in the range of 300-600 nm using Oriel 6365 150 W Xe-lamp and Oriel Cornerstone 7400 1/8 m monochromater. The IPCE value of the samples was calculated at each wavelength as follows:

$$IPCE (\%) = (j_{ph} \times \frac{h\nu}{p} \times \lambda) \times 100$$

where j_{ph} is the photocurrent density (mA/cm²), $h\nu$ is the photon energy of the incident light, ~ 1240 eV/nm, p is the power density of light (W/cm²), and λ is the irradiation wavelength (nm). The measurements were carried out in a 3-electrode setup, with an Ag/AgCl as the reference electrode, Pt as the counter electrode and the sample as the working electrode. 0.1 M Na₂SO₄ solution was used as the electrolyte.

Reflectance spectra were acquired using diffuse reflectance spectroscopy (DRS, Avantes AvaSpec-2048L spectrometer equipped with Avantes AvaLight-DH-S-BAL light source, Netherlands).

Photoluminescence spectra were collected in a back-scattering geometry, dispersed by an iHR320 monochromator (Horiba Jobin-Yvon), and recorded with a Peltier-cooled Si CCD (Synapse, Horiba Jobin-Yvon) using a laser of 375 nm.

Photocatalytic of H₂ evolution

The open-circuit H₂ evolution experiment was conducted under LED-light (wavelength: 365 nm, 180 mW/cm²) and with a magnetic stir bar (stir rate: 1000 rpm) in a quartz finger cell. The TiO₂ nanotubes were immersed in the mixture of water and methanol (10 %, as a hole capture agent). Long-term H₂ generation experiments were carried out at RT and at 50 °C in a solution containing different concentrations of H₂PtCl₆. For thermally annealed TiO₂ nanotubes, the H₂ generation activity was studied at ambient temperature and in a 10 % MeOH solution with 0.06 mM H₂PtCl₆. At regular intervals 200 μL of the gas in the head space of the reactor was taken and injected into a gas chromatograph (GCMS-QO2010SE chromatograph, SHIMADZU) to analyze the H₂ amount.

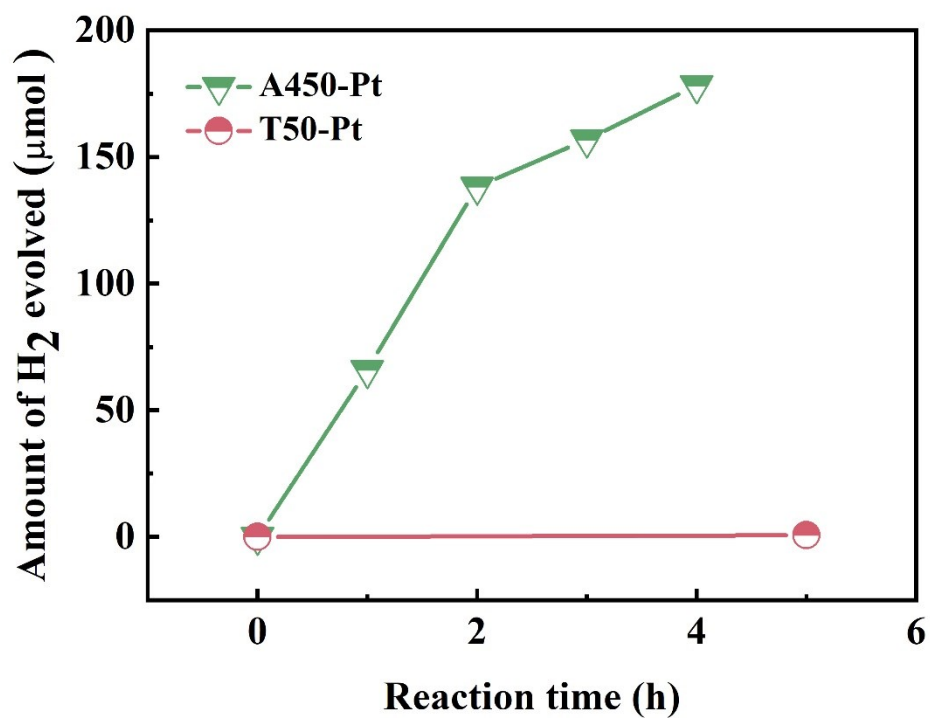


Fig. SI 1 Early stages of photocatalytic H₂ evolution of A450-Pt and T50-Pt

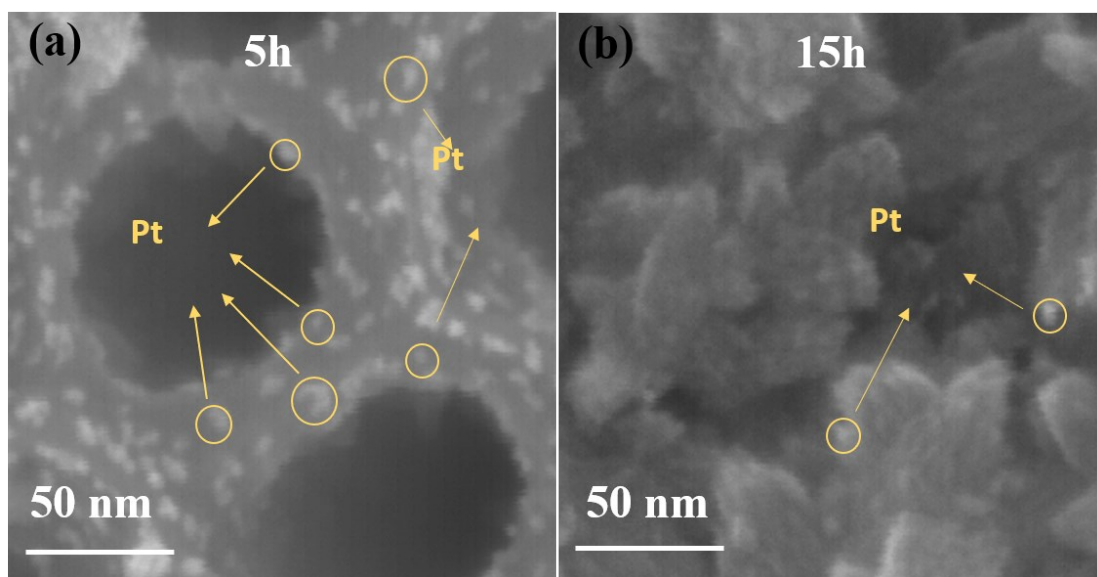


Fig SI 2 Top view of TiO₂ NTs after 5 h (a) and 15 h (b) of illumination and immersion.

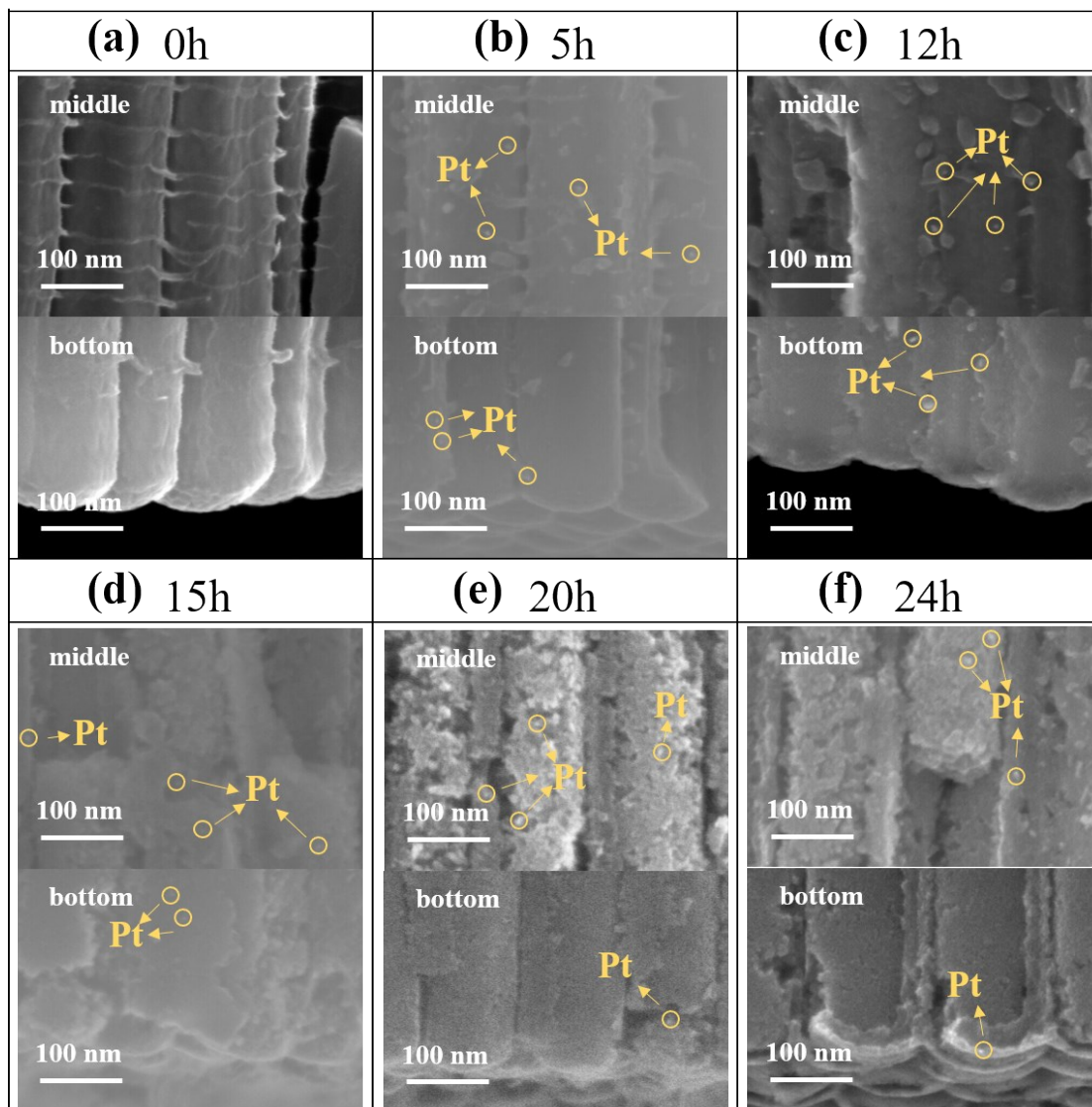


Fig. SI 3 SEM images of the middle and bottom of T50-Pt across photocatalytic H₂ generation.

The length of the tubes prepared is ca. 7 μm , while the electron diffusion length in TiO₂ NTs can be as long as 20-30 μm .¹ Therefore, electrons are available at the bottom of the tubes, where Pt⁴⁺ from Pt precursor can be reduced to Pt⁰ and deposited on the wall.

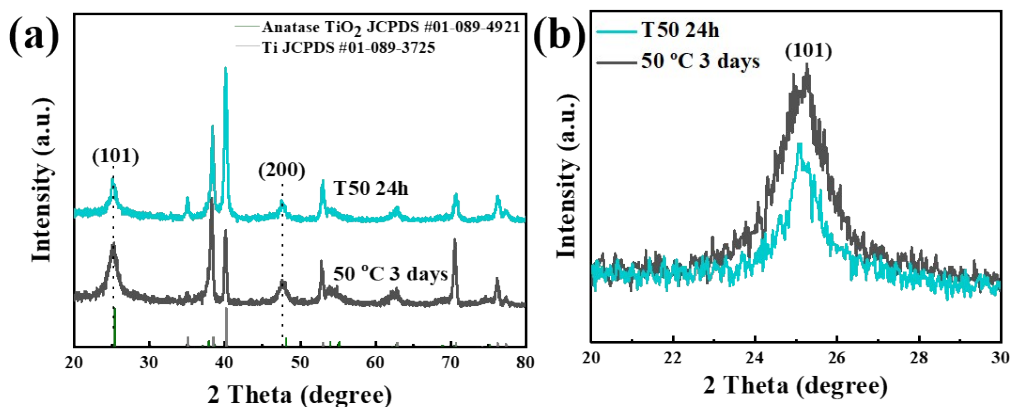


Fig. SI 4 XRD patterns for T50-24h and the tubes immersed in plain DI water in dark (no MeOH and Pt solution) at 50 °C for 3 days

The key to crystallization is the dissolution-crystallization process occurred when the amorphous TiO₂ NTs was immersed in aqueous solution. In this work, the main finding is the self-assembly of the photocatalyst during photocatalytic H₂ evolution (due to the in-situ crystallization and porosification of the nanotube walls).

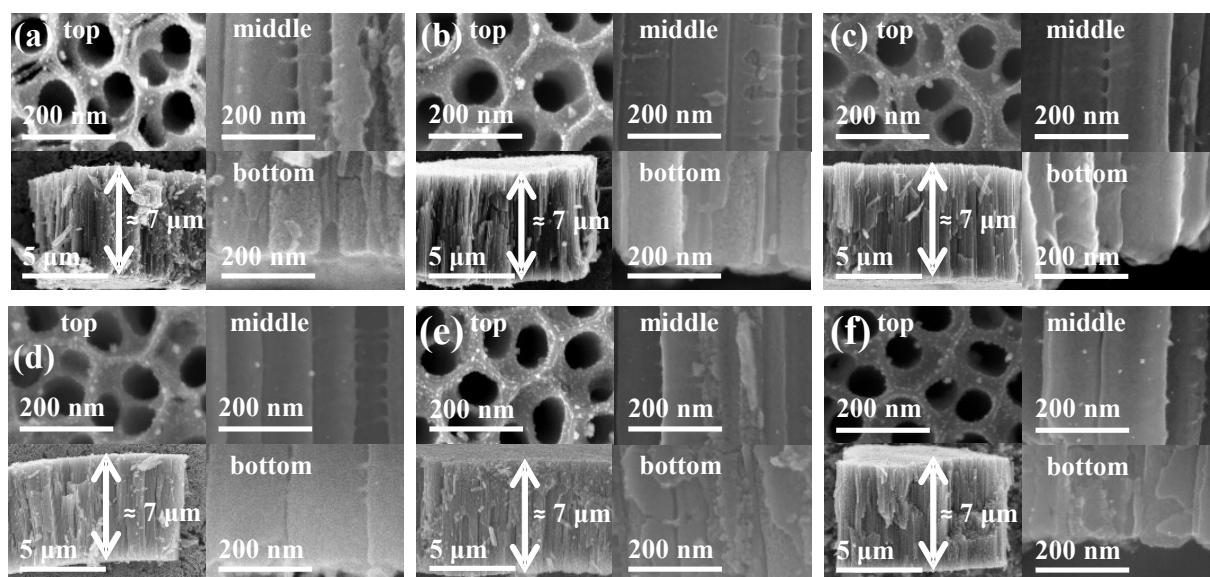


Fig. SI 5 SEM images of A450-Pt as a function of illumination time (a) 1 hour; (b) 2 hours; (c) 3 hours; (d) 4 hours; (e) 8 hours; and (f) 18 hours.

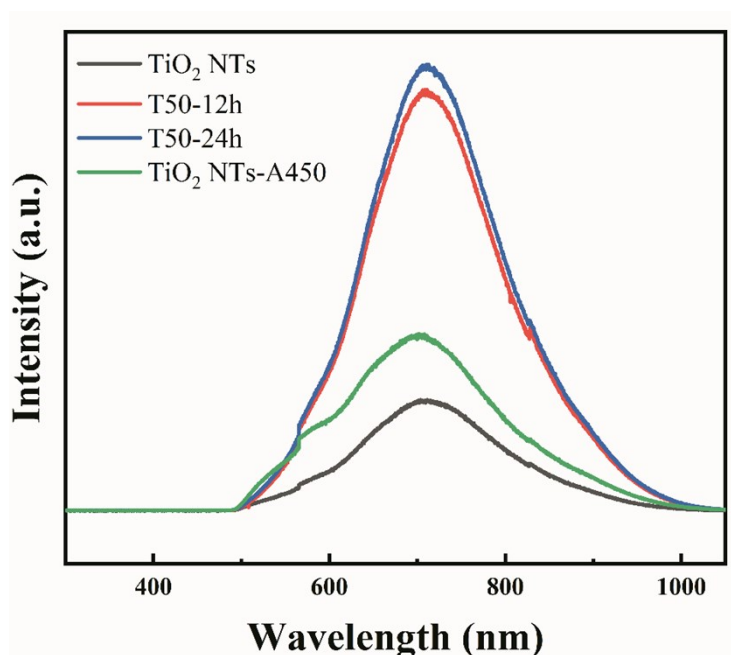


Fig. SI 6 PL spectra of amorphous TiO₂ NTs, T50-12h, T50-24h and TiO₂ NTs-A450.

The emission peak at ≈ 710 nm (that can be ascribed to a transition of trapped electrons to the valence band²) increases greatly likely due to the surface area increase during the crystallization process.³

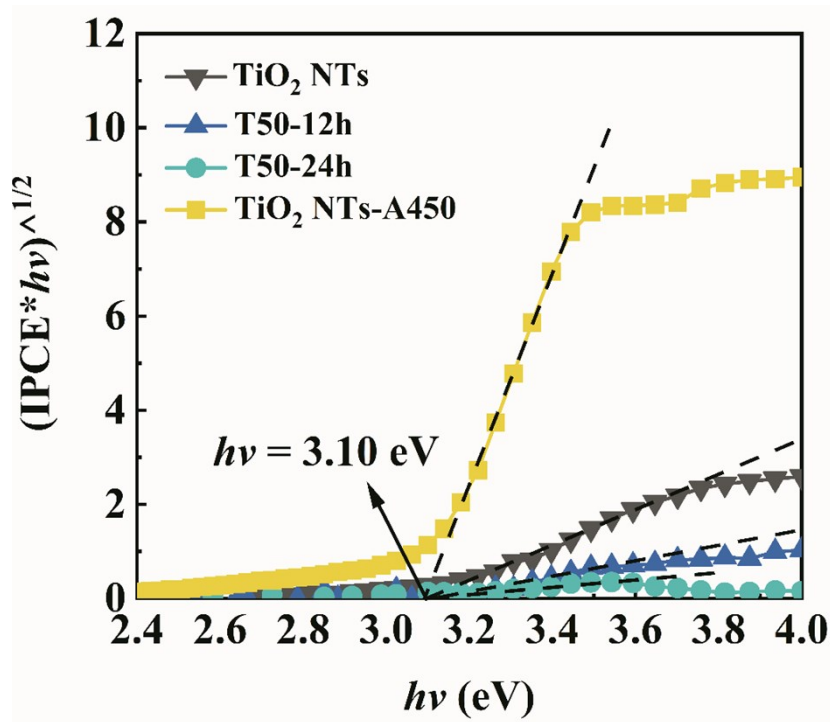


Fig. SI 7 Bandgap calculation of the amorphous TiO₂ NTs, T50-12h, T50-24h, and TiO₂ NTs-A450 samples based on the IPCE values.

Over exposure time amorphous TiO₂ becomes partially dissolved (see SEM in Fig. 2), also in line with previous capacitance measurements.³ This leads to a loss in connectivity and thus photoconductivity (magnitude of IPCE) – in other words, in spite of an increasing crystallinity the loss of connectivity dominates the photoresponse. This is in line with the increase of the PL peak at 710 nm that can be related to an increase of surface area, i.e. the trapping state related PL increases. Such surface states often have been described as beneficial for the photocatalytic activity.⁴

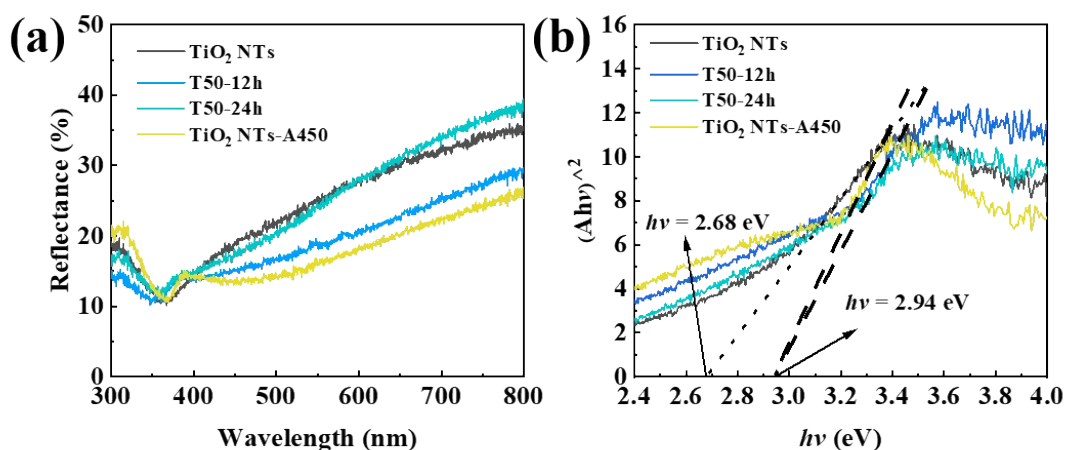


Fig. SI 8 Reflectance spectra of the amorphous TiO₂ NTs, T50-12h, T50-24h, and TiO₂ NTs-A450 (a) and the corresponding Tauc Plot $(A(h\nu))^2$ vs energy of the excited source (b).

We further determined bandgaps of the samples from photoelectrochemical and DRS measurements. While the results from photocurrent spectra show consistently a band (mobility) gap of 3.1 eV, the results from reflectance measurement show for the fresh amorphous tubes a sub-band gap contribution as typical for amorphous material.⁵ This supports further the notion of crystallization. As the crystallization processes based on dissolution-crystallization mechanism³ the drop of the photocurrent magnitude must be ascribed to a decrease in the coherent nanotube structure which leads to a drop in photoconductivity.

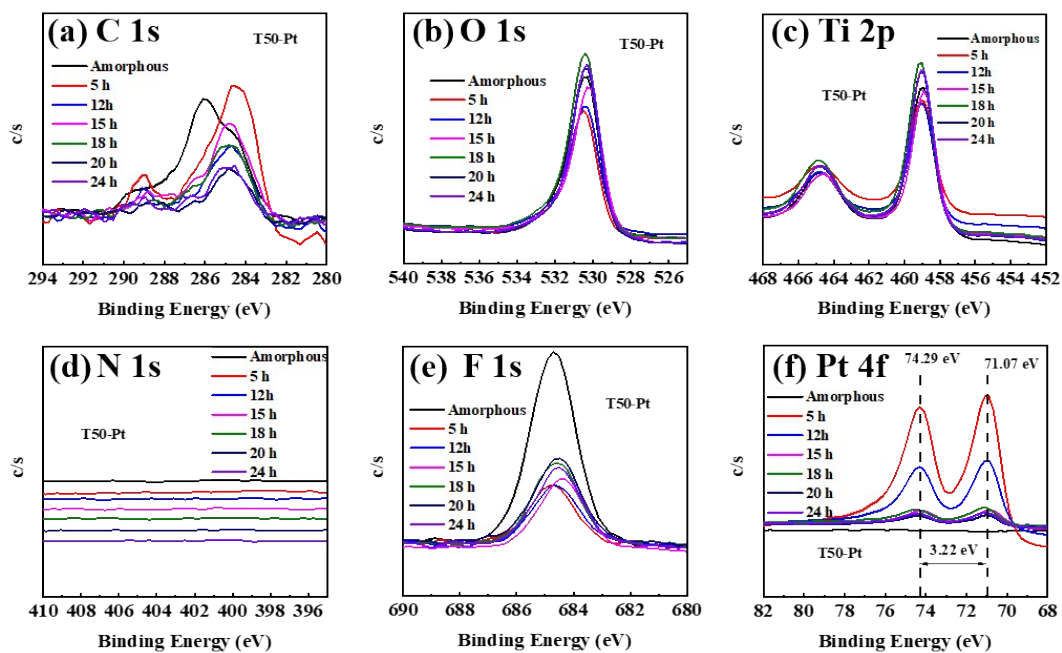


Fig. SI 9 High resolution XPS measurement of water annealing (0.05 mM Pt, 10 vol% methanol) TiO₂ nanotubes.

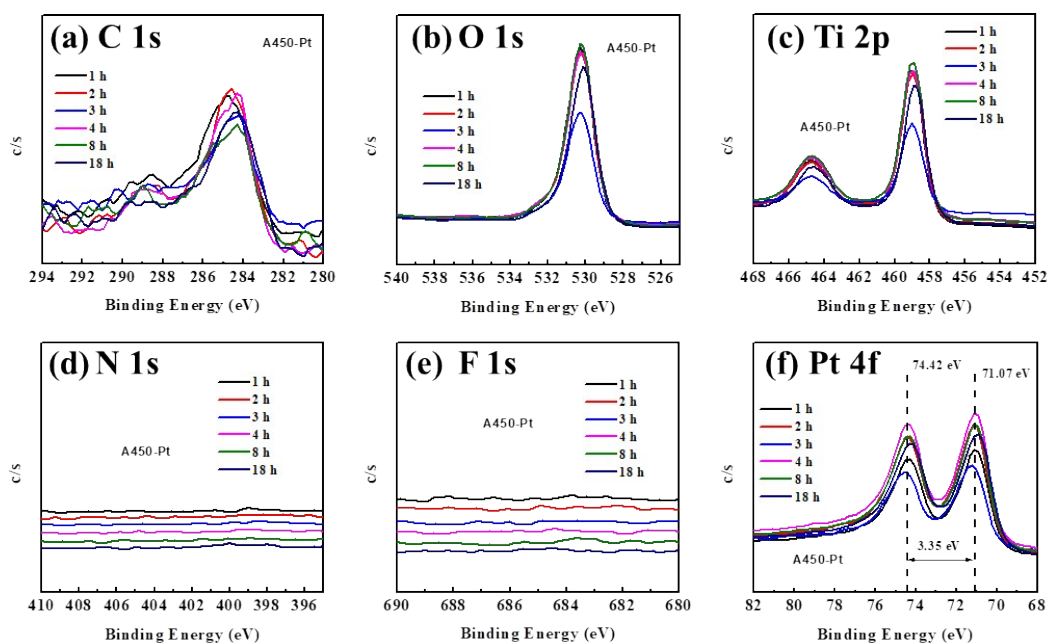


Fig. SI 10 High resolution XPS measurement of thermal annealed TiO₂ nanotubes soaking in the room temperature aqueous solution (0.05 mM Pt, 10 vol% methanol).

Table SI 1: EDX data of A450-Pt after a certain time of illumination, T50-0.005 mM Pt and T50-0.5 mM Pt after 24 hours of illumination.

Atom Concentration Table (at %)	C	O	Ti	F	Pt
A450-Pt 1 h	1.05	47.76	50.83	0	0.36
A450-Pt 2 h	1.68	46.97	50.96	0	0.39
A450-Pt 3 h	1.45	47.56	50.64	0.06	0.29
A450-Pt 4 h	1.78	47.32	50.45	0	0.45
A450-Pt 8 h	1.56	48.06	50.06	0	0.32
A450-Pt 18h	2.68	47.03	49.65	0.12	0.52
A450-Pt 5 h	6.34	45.69	43.34	4.16	0.47
A450-Pt 12 h	3.27	49.77	43.88	2.58	0.5
A450-Pt 15h	2.14	50.03	45.22	2.22	0.39
A450-Pt 20 h	2.22	51.16	43.81	2.59	0.22
A450-Pt 24h	1.75	51.39	44.14	2.43	0.29
T50-24h (0.5 mM Pt)	3.41	49.37	42.55	3.12	1.55
T50- 24h (0.005 mM Pt)	3.35	54.31	39.81	2.41	0.12

Table SI 2: XPS data of T50-Pt and A450-Pt throughout photocatalytic H₂ generation.

Atom Concentration Table (at %)	C 1s	O 1s	Ti 2p	F 1s	Pt 4f
Amorphous	9.79	53.02	23.33	13.84	0.03
A450-Pt 1 h	10.25	58.94	24.7	0.32	5.79
A450-Pt 2 h	10.07	58.31	23.9	0.51	7.22
A450-Pt 3 h	10.72	58.32	22.95	0.39	7.62
A450-Pt 4 h	10.86	57.94	23.64	0	7.55
A450-Pt 8 h	7.56	60.25	24.98	0.24	6.96
T50-5 h	14.07	52.28	20.02	5.11	8.52
T50-12 h	8.25	57.64	23.37	6.24	4.51
T50-15 h	8.91	58.26	24.99	5.81	1.02
T50-18 h	6.05	61.53	25.71	5.83	0.88
T50-20 h	3.79	62.63	26.19	6.79	0.6
T50-24 h	4.37	62.06	26.11	6.74	0.72

Reference

- 1 G. Cha, P. Schmuki and M. Altomare, *Electrochim. Acta*, 2017, **258**, 302.
- 2 D. K. Pallotti, L. Passoni, P. Maddalena, F. D. Fonzo, S. Lettieri, Stefano, *J. Phys. Chem. C*, 2017, **121**, 9011.
- 3 F. Fu, G. Cha, N. Denisov, Y. Chen, Y. Zhang and P. Schmuki, *ChemElectroChem*, 2020, **7**, 2792.
- 4 C. Gao, T. Wei, Y. Zhang, X. Song, Y. Huan, H. Liu, M. Zhao, J. Yu, and X. Chen, *Adv. Mater.*, 2019, **31**, 1806596.
- 5 C. Århammar, A. Pietzsch, N. Bock, E. Holmström, C. M. Araujo, J. Gråsjö, S. Zhao S. Green, T. Peery, F. Hennies, S. Amerioun, *Proc. Natl. Acad. Sci.*, 2011, **108**, 6355.